Online Resource 1

Limiter-aware reset control of the power synchronization loop for fault recovery of grid-forming inverters

Supplementary material for the article "Limiter-aware reset control of the power synchronization loop for fault recovery of grid-forming inverters", submitted to International Journal of Dynamics and Control. Author names and affiliation are withheld for double-blind review. Figures S1 to S8 and Tables S1 and S2 are cited in the main text. Equation, table, and section numbers without the prefix S refer to the main text.

S1. Loop shaping and describing function

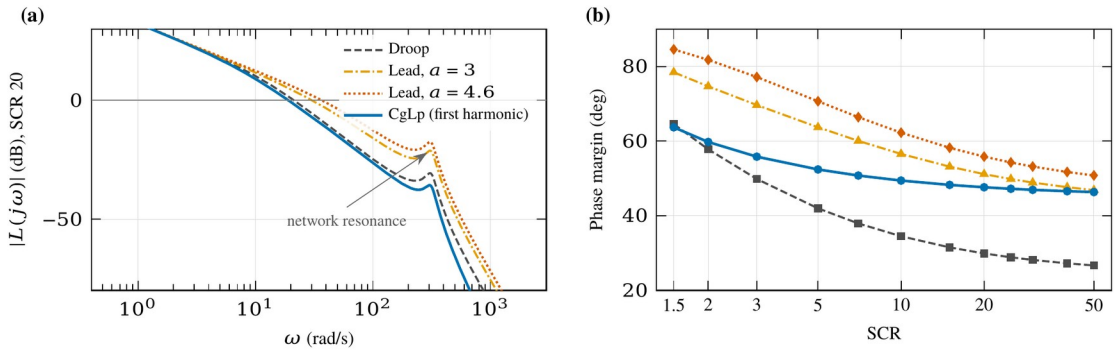

Fig. S1. (a) Open-loop gain |L(jω)| at SCR 20; the peak near 306 rad/s is the network resonance. (b) First-harmonic phase margin versus SCR.

At the crossover frequency ω_c = 21.3 rad/s the CgLp adds 16.7° of phase at a gain of 0.83. Its phase peaks at 24.5° near 51 rad/s, and its gain stays below unity above crossover: 0.55 at 50 Hz and 0.32 at 100 Hz. The leads with a = 3 and a = 4.6 add 29.6° and 39.5° at ω_c, with gains of 2.97

and 4.53 at 50 Hz. On a first-harmonic basis the CgLp loop therefore has less phase margin than the lead loops, although it stays 15 to 20° above plain droop for SCR 10 to 50.

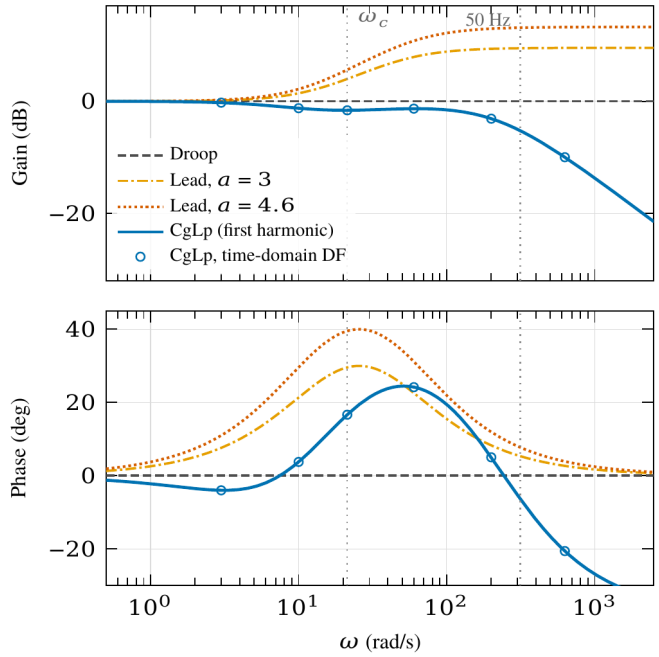

Fig. S2. First-harmonic gain and phase of the compensators. Lines: analytic describing function for the CgLp and exact frequency response for the leads. Circles: CgLp describing function extracted from time-domain simulation of the FORE.

S2. Common-rule tuning

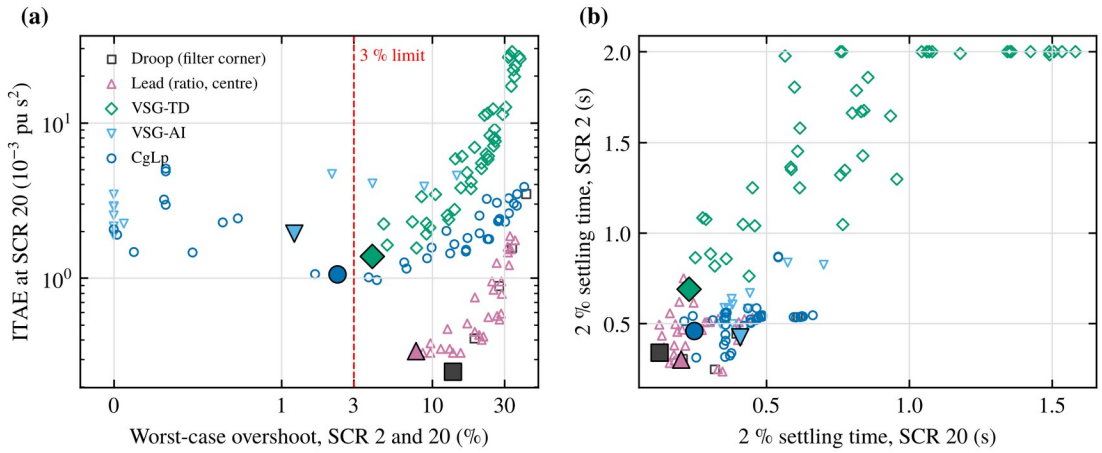

Fig. S3. Common-rule tuning of all controller families (132 designs): (a) ITAE at SCR 20 against the worst-case overshoot at SCR 2 and 20; (b) settling times at the two grid strengths. Filled markers: selected designs.

S3. High-frequency behavior of the averaged model

Table S1 reports the high-frequency behavior at SCR 20: the loop gain at 50 Hz, the frequency jitter under 0.02 p.u. white noise on the measured power, the 100 Hz ripple with 5 % negative-sequence grid voltage, and the step overshoot when a 2ω notch filters the measured power.

Table S1. High-frequency behavior at SCR 20 (averaged model).

Metric	Droop	Lead, a = 3	Lead, a = 4.6	Lead, re-tuned	VSG-TD	VSG-AI	CgLp
Gain at 50 Hz, |C(jω)|	1.00	2.97	4.53	7.28	n/a	n/a	0.55
RMS frequency jitter, noise 0.02 p.u. (mHz)	0.51 ± 0.05	0.81 ± 0.05	1.09 ± 0.06	1.24[a]	0.57[a]	0.53[a]	0.45 ± 0.03
100 Hz frequency ripple, V_n = 5 %, no notch (mHz p–p)	13.3	39.8	60.9	104.0	26.6	12.6	5.2
Step overshoot with V_n = 5 % and 2ω notch (%)	35.6	7.6	0.0	0.1	7.1	12.8	1.5

S4. Grid-code tests

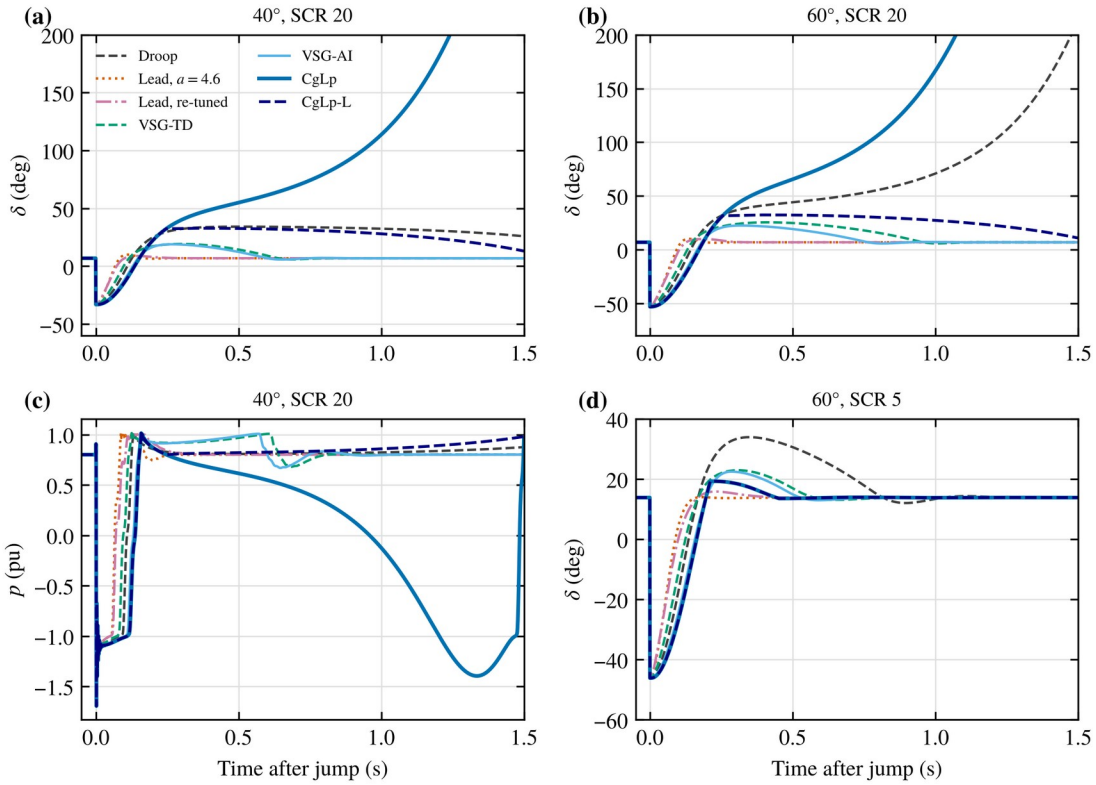

Fig. S4. Grid phase jumps (averaged model): angle after (a) 40° and (b) 60° jumps at SCR 20, (c) active power after the 40° jump at SCR 20, (d) angle after a 60° jump at SCR 5.

S5. Modified IEEE 9-bus system

Table S2. Complete multi-machine results for the nominal and weak (k_z = 2) networks.

Frequencies and powers on each unit's own base.

Units A and B	Network	SG nadir (Hz)	max $\lvert f_A - f_{SG} \rvert$ load step (mHz)	$p_{f,B}$ overshoot, B step (%)	max $\lvert \Delta p_A \rvert$ during B step (pu)	p_A recovery after fault (s)	max $\lvert f_A - f_{SG} \rvert$ fault (mHz)	p_A settling after trip (s)
Droop	nominal	49.934	19.9	48.2	0.076	0.82	454	1.71
Lead, a = 4.6	nominal	49.929	29.6	23.1	0.090	0.81	635	1.84
Lead, re-tuned	nominal	49.931	25.6	26.1	0.085	0.81	573	1.81
VSG-	nominal	49.934	18.8	24.1	0.071	0.84	479	1.74

Units A and B	Network	SG nadir (Hz)	max $\lvert f_A - f_{SG} \rvert$ load step (mHz)	$p_{f,B}$ overshoot, B step (%)	max $\lvert \Delta p_A \rvert$ during B step (pu)	p_A recovery after fault (s)	max $\lvert f_A - f_{SG} \rvert$ fault (mHz)	p_A settling after trip (s)
TD								
VSG-AI	nominal	49.936	18.1	23.7	0.071	0.73	377	1.75
CgLp	nominal	49.937	18.0	25.1	0.076	0.31	366	2.29
CgLp-L	nominal	49.937	18.0	25.1	0.076	0.29	366	2.29
CgLp + Droop	nominal	49.935	19.2	52.5	0.083	0.31	365	2.27
CgLp + VSG-AI	nominal	49.937	18.3	24.2	0.073	0.31	365	2.29
Droop + CgLp	nominal	49.935	18.2	22.3	0.070	0.83	454	1.72
Droop	weak (×2)	49.941	21.6	35.2	0.074	0.96	481	2.32
Lead, a = 4.6	weak (×2)	49.938	22.1	17.2	0.072	0.91	682	2.23
Lead, re-tuned	weak (×2)	49.939	22.0	19.5	0.073	0.93	612	2.26
VSG-TD	weak (×2)	49.941	21.4	19.8	0.073	0.96	509	2.33
VSG-AI	weak (×2)	49.944	20.6	19.4	0.072	0.36	394	2.37
CgLp	weak (×2)	49.944	20.4	26.1	0.075	0.30	381	2.46
CgLp-L	weak (×2)	49.944	20.4	26.1	0.075	0.27	381	2.46
CgLp + Droop	weak (×2)	49.943	20.9	38.8	0.076	0.29	380	2.44
CgLp + VSG-AI	weak (×2)	49.944	20.5	19.7	0.073	0.29	380	2.42
Droop + CgLp	weak (×2)	49.943	20.9	24.9	0.071	0.98	482	2.35

S6. Additional averaged-model responses

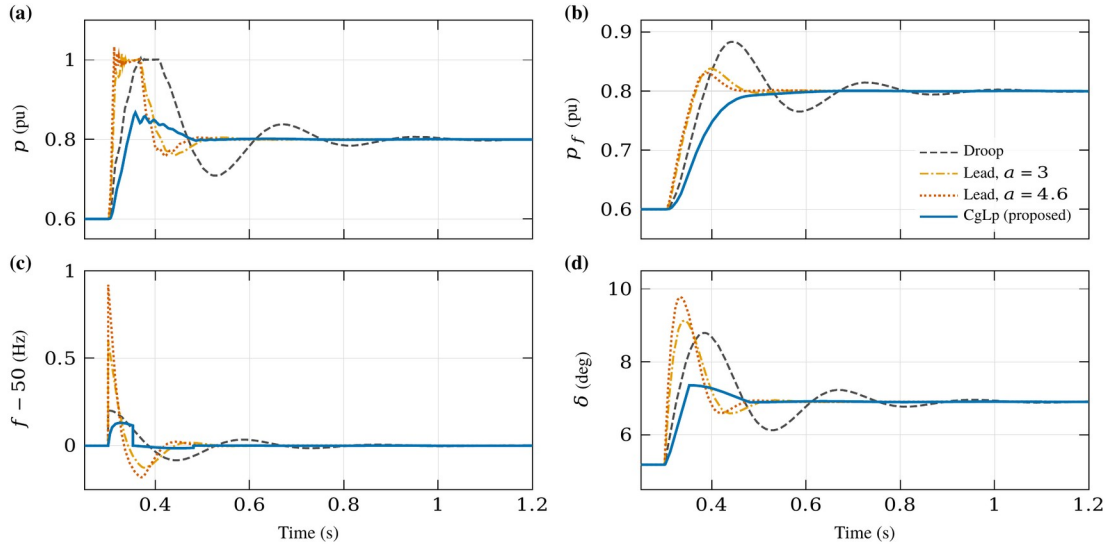

Fig. S5. Power step 0.6 → 0.8 p.u. at SCR 20 (averaged model): (a) instantaneous power, (b) filtered power, (c) internal frequency deviation, (d) angle $\delta = \theta - \theta_g$.

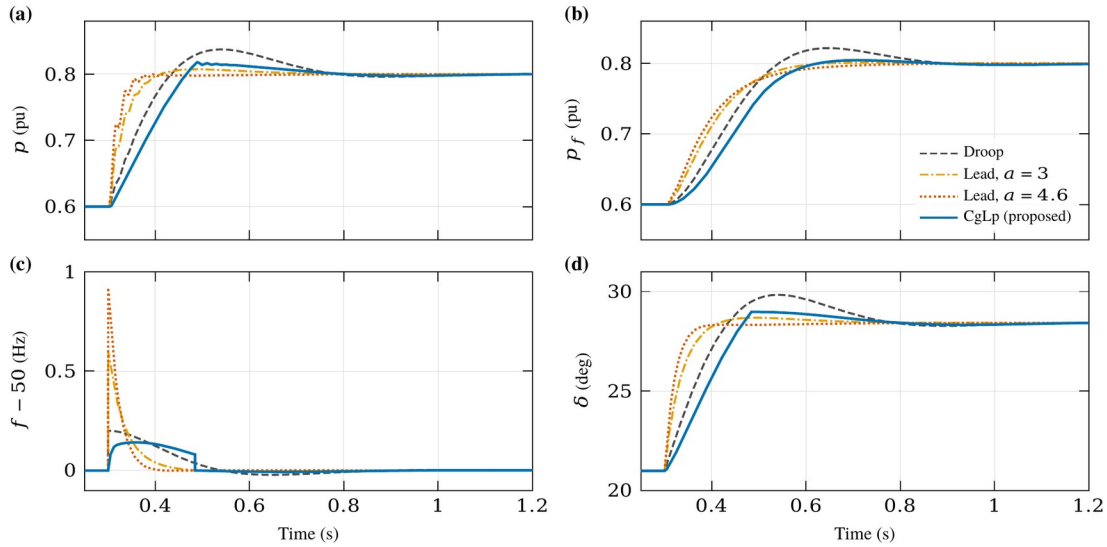

Fig. S6. Power step 0.6 → 0.8 p.u. at SCR 2 (averaged model): (a) instantaneous power, (b) filtered power, (c) internal frequency deviation, (d) angle.

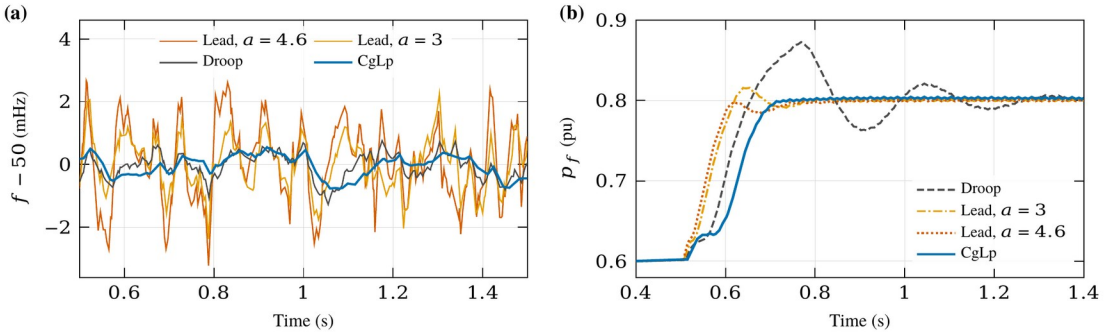

Fig. S7. (a) Internal frequency deviation under measurement noise at SCR 20 (one realization). (b) Power step with 5 % negative-sequence voltage and a 2ω notch on the measured power.

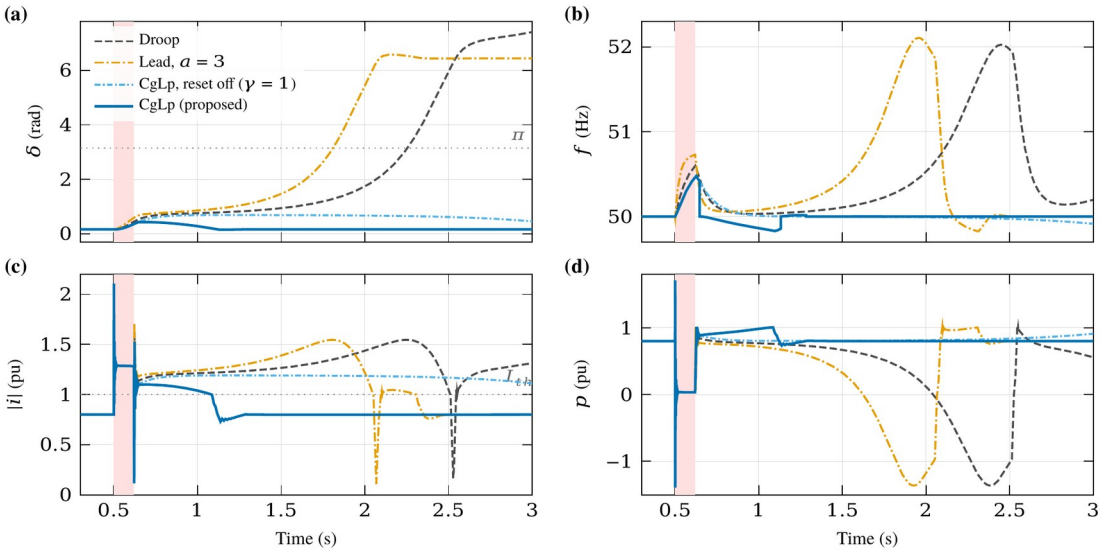

Fig. S8. 120 ms bolted dip at SCR 10 (shaded interval), averaged model: (a) angle, (b) frequency, (c) current magnitude, (d) active power.